

Article

A Theoretical Analysis of Meteorological Data as a Road towards Optimizing Wind Energy Generation

Olga Orynych^{1,*}, Paweł Ruchała², Karol Tucki^{3,*}, Andrzej Wasiak⁴ and Máté Zöldy⁵

¹ Department of Production Management, Faculty of Engineering Management, Białystok University of Technology, Wiejska Street 45A, 15-351 Białystok, Poland

² Aerodynamics Department, Łukasiewicz Research Network—Institute of Aviation, Al. Krakowska 110/114, 02-256 Warszawa, Poland; pawel.ruchala@ilot.lukasiewicz.gov.pl

³ Department of Production Engineering, Institute of Mechanical Engineering, Warsaw University of Life Sciences, Nowoursynowska Street 164, 02-787 Warsaw, Poland

⁴ Advisors Panel Production Engineering, Alternative Energy Sources Białystok, 15-351 Białystok, Poland; andrzej.wasiak@gmail.com

⁵ Department of Automotive Technologies, Budapest University of Technology and Economics, Műegyetem rkp. 3., 1111 Budapest, Hungary; zoldy.mate@kjk.bme.hu

* Correspondence: o.orynych@pb.edu.pl (O.O.); karol_tucki@sggw.edu.pl (K.T.); Tel.: +48-746-98-40 (O.O.); +48-593-45-78 (K.T.)

Abstract: The development of wind energy has been observed for many years. Both construction firms and the scientific world are analyzing new design solutions, atmospheric conditions and the technical performance achieved. The main goal of this research is to evaluate the requirements that have to be met to design wind power stations that would be an optimal fit for the climatic conditions in Poland. This study combines the results of empirical studies on wind velocity distributions with the physical fundamentals of wind power station design. This paper presents modelling of the relationships between wind velocity distributions observed in Poland and technical requirements for wind power stations design. The wind velocities distributions for various locations in Poland are determined and expressed in Weibull distribution parameters. Theoretical computations concerning the dependence of wind power stations as function of wind speed and air's physical properties are presented. Conclusions important for the design of power stations fitted to the atmospheric conditions in Poland are given. LabVIEW 2021 was used for computer modeling.

Keywords: wind turbine; energy; turbine efficiency; power; calculation



Citation: Orynych, O.; Ruchała, P.; Tucki, K.; Wasiak, A.; Zöldy, M. A Theoretical Analysis of Meteorological Data as a Road towards Optimizing Wind Energy Generation. *Energies* **2024**, *17*, 2765. <https://doi.org/10.3390/en17112765>

Academic Editor: Adrian Ilinca

Received: 21 April 2024

Revised: 31 May 2024

Accepted: 2 June 2024

Published: 5 June 2024



Copyright: © 2024 by the authors. Licensee MDPI, Basel, Switzerland. This article is an open access article distributed under the terms and conditions of the Creative Commons Attribution (CC BY) license (<https://creativecommons.org/licenses/by/4.0/>).

1. Introduction

The energy transition of European Union member states has been observed for many years. Ambitious targets for reducing CO₂ emissions are influenced by historical circumstances, geopolitical location and climatic conditions. Developing and promoting renewable energy is one of the ways to achieve the EU's climate goals. With the increase in RES (renewable energy source) capacity, the management of electricity systems is becoming an increasing challenge [1].

The energy policy and environmental policy of the European Union (EU) has for years had an impact on renewable energy [2]. Renewable energy sources are a starting point of many debates between European politics, representatives of energy companies, scientists and consumers [3–5]. According to the findings of the European Parliament, by 2030, renewable energy sources must make up at least 40% of energy consumed within the EU, which has led to the reduction in greenhouse gases up to 55% in comparison to 1990. The internal law regulations of EU members strongly underline a need for acceleration of energy market structure transformation [6,7].

In 2023, 55 percent of electric energy in Germany was created by renewable energy sources. The majority of this production was from in-land wind turbines. All these wind

turbines, both in-land and seashore, made up 31.1% of the produced electric energy [8]. In the same year, Portugal generated even greater amounts of electric energy coming from renewable energy sources: up to 61%, a quarter of which came from wind energy. Noticeably, just a year before (in 2022), the amount of renewable energy sources in the total production of electric energy in Portugal was 49% [9].

According to PSE (Polskie Sieci Elektroenergetyczne—Polish Electricity Networks) data, the amount of coal energy in 2023 has been reduced to 63%, the amount of renewable energy sources has been increased to 27% and the amount of gas energy is 10%. The total power of all installed wind farms was 9428.3 MW (end of December, 2023). Moreover, Polish seashore wind turbines—both developed in Poland and abroad—are currently being planned, which should achieve a power of 5.9 MW by 2030 and 11 MW by 2040. The Energy Policy of Poland of 2040 defines the building and development of seashore wind farms as a strategic direction of the energy market transformation, which enforces energy safety and drives the economic development of Poland [10].

By 2024, 43 percent of the generating capacity for electricity production in Poland will be from renewable energy sources. The 50% threshold could be exceeded this year, and in ten years it could be over 70%.

Over the years, one may have observed the progression of the design and technology used in wind turbines, both seashore and in-land. For instance, the Dutch start-up company TouchWind proposes a concept of single-bladed wind turbines, Mono. The advantages of such a concept are, amongst others, a lower mass and a wide range of wind speed when the turbine works effectively. Furthermore, the manufacturing cost of such a turbine may even be 30–50% of similar value for typical, three-bladed wind turbines. The latter has been achieved due to the simplicity of both the rotor and its base [11].

At the end of 2020, the company Vestas introduced the V155-3.3 MW wind turbine, as a variation of 4 MW platform, developed to utilize weak and ultra-weak wind. Similarly, version V155-3.6 MW has been modernized and technically optimized to extend the possibility of application. Such a turbine is aimed to be offered to locations where the dominant wind speed is low—including India, the USA and many countries in Europe and Latin America [12].

The Norwegian start-up World Wide Wind started the testing their prototype of a floating wind turbine, equipped with a pair of contra-rotating, vertical axis rotors. The power of the prototype is only 30 kW. The electric generator is located on the bottom—below the water surface—as a stabilizer and a contra-balance. The rotor blades move along a three-dimensional curves and additional supports increase the efficiency of wind energy capture. The concept allows the distance between adjacent turbines within the wind farm to be reduced up to 50% [13].

Moreover, at Northwester 2 wind farm, the MHI Vestas company has installed a prototype of the turbine with a power of 9.5 MW, rotor dimension of 174 m and blade length of 85 m.

Another prototype, developed by GE Renewable Energy, is a Haliade-X wind turbine with an output power of 12 MW. It is estimated that for wind conditions typical for the German part of the Northern Sea, the outcome of electric energy may reach up to 67 GWh per year. This turbine may be compared to Cypress, another turbine family produced by GE Renewable Energy. The Cypress is an in-land wind turbine with a power of 5.3 MW and rotor diameter of approximately 160 m. Its prototype has been installed in Wieringermeer (Holland) and started its operational phase in February, 2019 [14,15].

Also, Siemens Gamesa has developed an offshore wind turbine, with a power of 14 MW. According to the manufacturer, it has a rotor diameter of 222 m, blade length of 108 m and hub weight of 500 tons. The same company, Siemens Gamesa, has also developed a concept for energy storage, that utilizes wind turbines and volcanic stones heated up to 600 degrees Celsius using the energy collected by the wind turbine. The heated stones are stored in the isolated sarcophagus and may be cooled when the wind turbine is off. In this way, vapor is produced to power the turbine [16].

Construction materials are the subject of scientific research. Wind turbine designers need to solve the problem of excessive vibration in conventional steel tube towers [17].

An example of a different approach is the Polish wind turbine VENTUS Power Generator [18,19]. Such a turbine is designed as an extremely small device used by a single household. The company offers three-bladed HAWT turbines that create the Y-type family: Ventus 500 W, Ventus 1000 W and Ventus 2000 W. The design is based on the FD family developed in Canada, but the tail shape and blades airfoil have been implemented to shift the optimum efficiency point to wind speeds between 4.5 m/s and 6.5 m/s, which are the most common values that appear in Poland. A key factor during optimization was low noise and mass, as well as high reliability [20,21].

The main aim of the present research is to evaluate the requirements that have to be met to design wind power stations that would be an optimal fit for the climatic conditions in Poland. This study combines the results of empirical studies on wind velocity distributions with the physical fundamentals of wind power station design. The modelling of relationships among wind velocity distributions observed in Poland gives us a tool for the discussion and evaluation of the technical requirements for wind power station design. The wind velocity distributions for various locations in Poland are determined and expressed in Weibull distribution parameters. Theoretical computations concerning the dependence of wind power stations as a function of wind velocity and air physical properties are presented. Conclusions important for the design of power stations corresponding to atmospheric conditions in Poland are given.

2. Materials and Methods

In general, the energy generated by wind turbines obviously depends on wind velocity and turbine efficiency (which is a function of wind velocity).

Wind velocity may be described with velocity magnitude and wind direction. The latter parameter should be immaterial for the wind turbines. HAWTs (Horizontal Axis Wind Turbines), which are the most common wind turbines utilized in Poland, achieve this feature through rotation along the vertical mast that aligns the rotation axis with the wind. Other turbine types may achieve independence from the wind direction in different ways, for instance, VAWT (Vertical Axis Wind Turbines–Savonius-type, Darrieus-type, etc.) have a vertical axis of symmetry. Eventually, the energy of a wind turbine is a function of its efficiency and the wind velocity magnitude. Extremely strong wind may achieve nearly 50 m/s of speed, but with relatively small probability: around 95% of winds are less than 47 m/s. In this range of wind speeds, the cumulative probability of the wind maximum speed can be approximated using a simple, single-equation Gumbel distribution [22–24]:

$$F(V_k) = \exp\{-\exp[-(V_k - 32.4)/5.14]\} \quad (1)$$

The relation presented above shows the maximum speed independent of direction. The meteorological data processed and presented by Żurański and Jaśpińska in [22] clearly showed that in the whole lowland part of Poland, the strongest winds come from the western direction. The dynamic pressure of eastern and southern winds can be reduced twice. On the other hand, the maximum wind speed is crucial in terms of the strength of the wind turbine, but not so much in terms of the assessment of its energy [25,26]. Clearly, each turbine works when the wind speed is in its respective threshold: above the lowest wind speed, which may move the turbine's rotor, and below the maximum permitted speed, determined by the blades' strength. It is thus necessary to know the distribution of wind speed probability density. For years, researchers have agreed that such distributions may be well defined using the Weibull distribution [27,28] despite its limitations, e.g., having a purely empirical basis, which leads to the omission of physical relations that would determine the wind speed [29]. As a result of the abovementioned limitations, some new statistical models have been developed to improve the fitting of the wind speed parent data, including the Offset Elliptical Normal (OEN) model applied in [30] or a combination of three models (the Kappa distribution, Wakeby distribution and Burr-Generalized Extreme

Value distribution) proposed in [31]. The results of such studies promise a better overall accuracy of parent data fitting compared to the Weibull distribution. On the other hand, a novel approach is a tool which has not been widely utilized yet; thus, using the well-known Weibull distribution allows us to employ previously generated data.

In the Weibull distribution, the probability of a given wind speed V can be expressed with the following formula [2,3]:

$$f(V) = \frac{k}{c} \left(\frac{V}{c}\right)^{k-1} \cdot \exp\left(-\left(\frac{V}{c}\right)^k\right) \quad (2)$$

where k —shape parameter, c —scale parameter, and V —wind speed.

The cumulative probability function may be given with the following expression:

$$F(V) = 1 - \exp\left(-\left(\frac{V}{c}\right)^k\right) \quad (3)$$

This function describes the probability that the wind speed is less or equal to V .

To determine the probability distribution of the speed, it is crucial to define the shape parameter k and the scale parameter c . We performed this based on the meteorological data gathered by each synoptical station in Poland in 2023, written in SYNOP reports [4]. Each station recorded data (amongst others, the wind speed) hourly. An exemplary histogram of the wind speed (determined for the Łódź station) has been presented in Figure 1. Clearly, one can observe that the histogram shape resembles a Weibull distribution, with a most probable (most commonly observed) value of about 2 m/s.

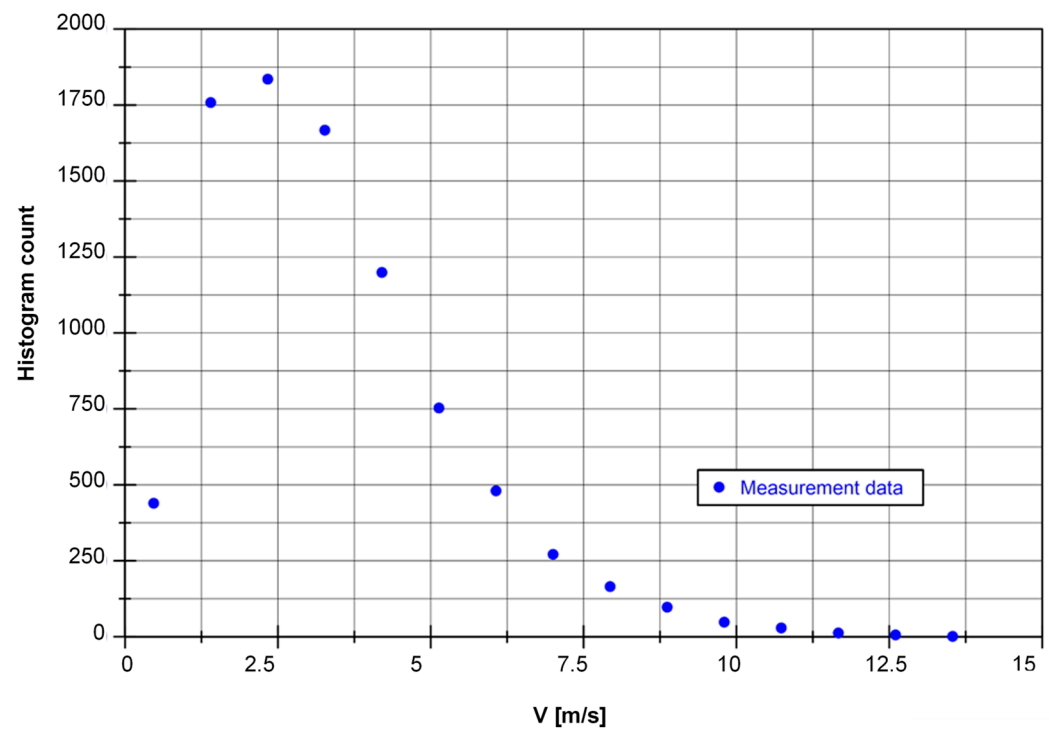


Figure 1. Exemplary histogram of wind speed.

Determination of the coefficient defining the Weibull distribution is a crucial task at this moment. The research community applies several methods, defined and described in a detailed manner, e.g., in [2,3,5], among others: the moment method, graphical method, empirical method, maximum likelihood method, modified maximum likelihood method, and energy pattern factor method.

The selection of a method must include the size of the available data, as well as its form, i.e., whether it is a time-series or a histogram form. As the data used in the following study have been logged as a time-series, to determine the Weibull parameters, the maximum likelihood estimation (MLE) has been exploited [2,3,6]. It is also the most promising method, according to the comparison performed in [5].

Within the MLE method, the shape parameter is given with the following equation:

$$k = \left(\frac{\sum_{i=1}^n [V_i^k \cdot \ln(V_i)]}{\sum_{i=1}^n V_i^k} - \frac{\sum_{i=1}^n \ln(V_i)}{n} \right)^{-1} \quad (4)$$

$$c = \left(\frac{1}{n} \sum_{i=1}^n V_i^k \right)^{1/k} \quad (5)$$

where V_i —wind speed in the i -th sample and n —the number of samples.

The first of these equations must be solved iteratively, as the wind speed in k -th power appears on its right side. The initial value of $k = 2$ has been assessed, as suggested in [3]. The LabVIEW diagram of calculations has been presented in Figure 2.

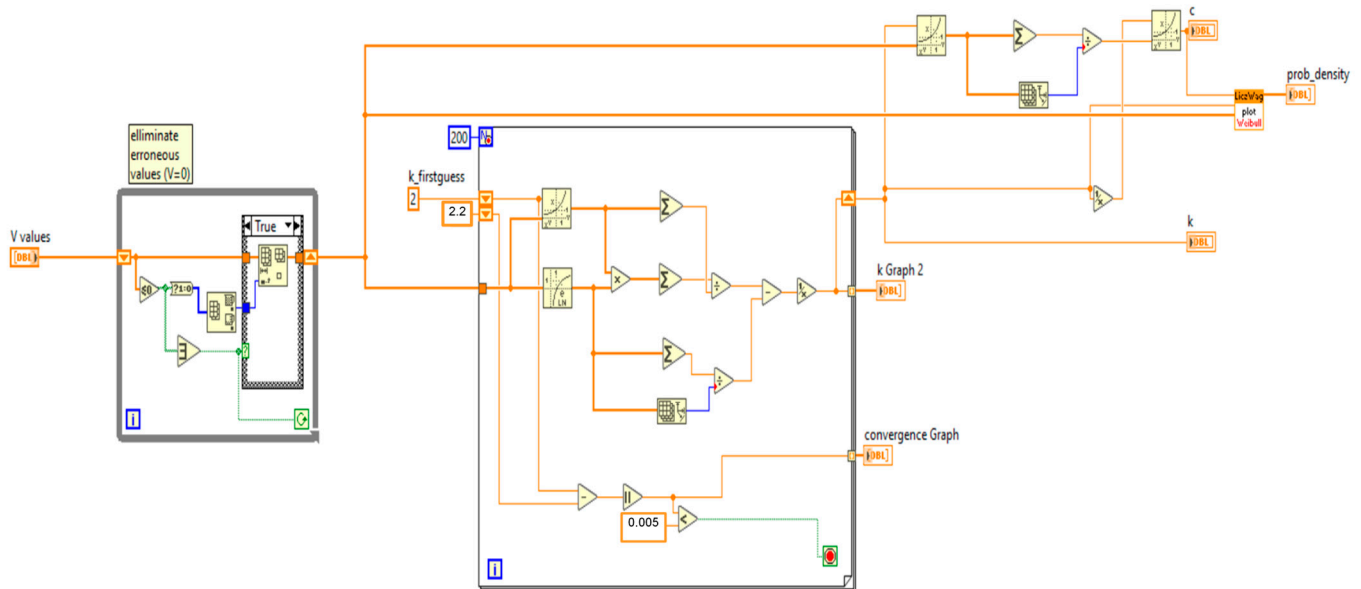


Figure 2. LabVIEW diagram of MLE method.

The quality of assessment of the Weibull distribution is satisfactory, as it has been presented in Figure 3, where the cumulative probability function has been presented for a randomly chosen station (Łódź—same as in Figure 1). However, a slight underestimation of moderate wind speeds may be observed.

The wind speed data included in SYNOP reports are gathered by the anemometer located at a relatively small height above ground level: roughly 10 m (depending on the station). Meanwhile, wind turbines utilize the wind at much greater heights. Thus, the wind energy has been assessed at the height of 100 m, which is a promising value according to the trends presented in the Introduction Section. The wind speed increases with height, and this relation is commonly described using Hellman's exponential law [32,33]:

$$\frac{V_1}{V_2} = \left(\frac{H_1}{H_2} \right)^\alpha \quad (6)$$

where the coefficient α depends on the surroundings of the wind turbine, as it modifies the shear layer of the wind. This effect can be compared with the impact of the surface roughness on the boundary layer thickness when the fluid flows along this surface. To determine the exponent α , it is convenient to define some categories of the terrain: it is clearly expected that in a clear area, like a seashore, the shear layer will be much thinner than in densely populated cities. In Poland (as in other EU countries), the terrain categories and respective exponents are proposed by the architectural standard PN-EN 1991-1-4:2008 with its national annex (Tables 1 and 2) [33]. The categories have been summarized in Table 2. In the presented study, the value of $\alpha = 0.17$ has been set, which, according to Polish standards [8], represents an open terrain with low vegetation and isolated obstacles like trees or houses (II category); see Table 1.

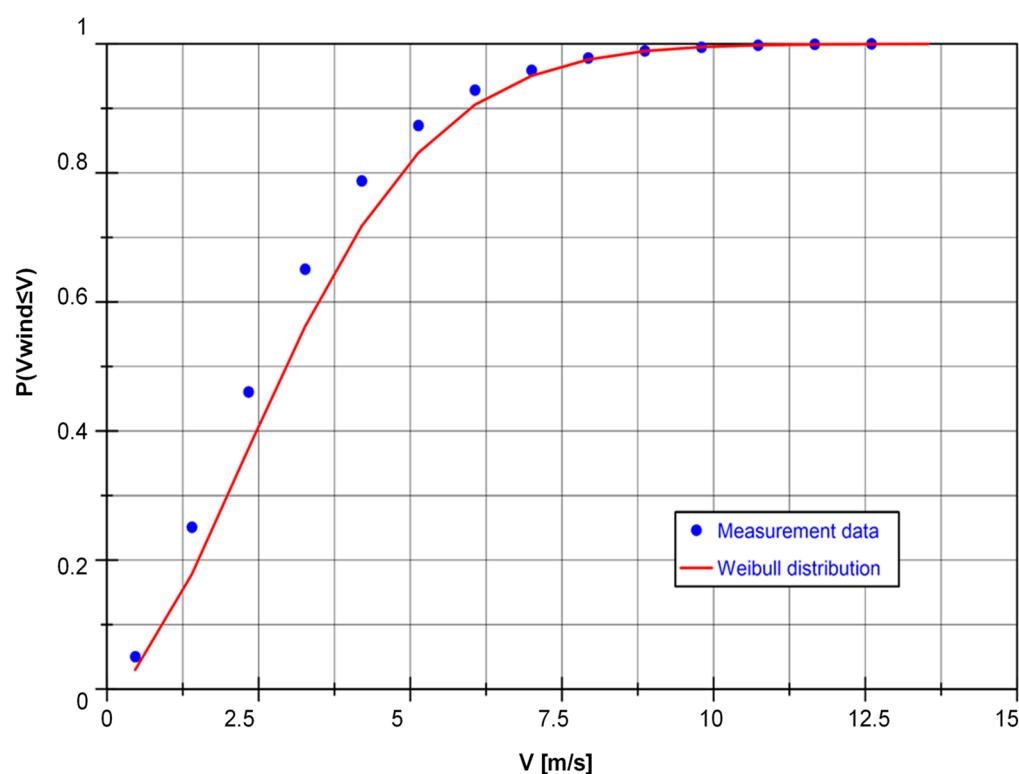


Figure 3. Cumulative probability of wind speed, according to raw data and Weibull estimation.

Table 1. Impact of height on wind turbine power, depending on terrain category.

| Terrain Class | Terrain | alpha |
|---------------|--|-------|
| 0 | Sea and coastal area exposed to the open sea | 0.11 |
| I | Lakes or area with negligible vegetation and without obstacles | 0.13 |
| II | Area with a low vegetation, such as grass and isolated obstacles (trees, buildings) with separations of at least 20 obstacle heights | 0.17 |
| III | Area with regular cover of vegetation or buildings or with isolated obstacles with separation of max. 20 obstacle heights (e.g., villages, suburbia, permanent forest) | 0.19 |

Table 2. Calculated WPD values for various stations with coefficients of Weibull distribution and geographic position.

| Station | Longitude (E) | Latitude (N) | H _{station} ASL | H _{anemometer} AGL | c | k | V _{average} | V _{max gust} | WPD |
|---------------------|---------------|--------------|--------------------------|-----------------------------|-------|-------|----------------------|-----------------------|---------------------|
| - | [°] | [°] | [m] | [m] | [m/s] | [-] | [m/s] | [m/s] | [W/m ²] |
| Kołobrzeg-Dźwirzyno | 15.389 | 54.158 | 4 | 11 | 8.53 | 1.779 | 7.59 | 29 | 591.35 |
| Łeba | 17.535 | 54.754 | 1 | 22.7 | 7.713 | 1.798 | 6.859 | 29 | 431.69 |
| Ustka | 16.854 | 54.588 | 3 | 22.7 | 7.758 | 1.877 | 6.887 | 28 | 415.50 |
| Zamość | 23.206 | 50.698 | 223 | 11 | 6.931 | 1.831 | 6.159 | 50 | 298.33 |
| Rzeszów-Jasionka | 22.042 | 50.111 | 206 | 10 | 6.585 | 1.814 | 5.854 | 27 | 258.62 |
| Kraków-Balice | 19.802 | 50.080 | 236 | 10 | 6.405 | 1.767 | 5.702 | 21 | 245.81 |
| Elbląg-Milejewo | 19.544 | 54.223 | 189 | 10 | 6.737 | 2.053 | 5.968 | 20 | 242.44 |
| Poznań-Ławica | 16.836 | 52.417 | 88 | 10 | 6.628 | 1.977 | 5.875 | 21 | 241.54 |
| Kalisz | 18.082 | 51.782 | 137 | 10 | 6.543 | 1.969 | 5.801 | 19 | 232.08 |
| Świnoujście | 14.242 | 53.923 | 4 | 20 | 6.175 | 1.836 | 5.486 | 26 | 215.06 |
| Kętrzyn | 21.369 | 54.068 | 107 | 10 | 6.075 | 1.773 | 5.407 | 21 | 212.05 |
| Bielsko-Biała | 19.001 | 49.808 | 396 | 14.2 | 5.928 | 1.704 | 5.288 | 25 | 201.16 |
| Racibórz | 18.192 | 50.062 | 206 | 10 | 5.808 | 1.706 | 5.181 | 23 | 193.12 |
| Włodawa | 23.529 | 51.553 | 177 | 12 | 6.194 | 2.027 | 5.488 | 23 | 190.54 |
| Kłodzko | 16.614 | 50.437 | 356 | 10 | 5.344 | 1.482 | 4.831 | 23 | 187.33 |
| Łódź-Lublinek | 19.400 | 51.723 | 174 | 10 | 5.665 | 1.697 | 5.055 | 22 | 181.33 |
| Hala Gąsienicowa | 20.006 | 49.244 | 1523 | 10.4 | 5.593 | 1.53 | 5.038 | 32 | 179.28 |
| Gdańsk-Świbno | 18.934 | 54.334 | 7 | 20.2 | 6.028 | 2.036 | 5.341 | 24 | 178.24 |
| Sulejów | 19.864 | 51.353 | 188 | 11 | 5.671 | 1.733 | 5.054 | 22 | 176.44 |
| Koszalin | 16.156 | 54.204 | 33 | 10.5 | 5.807 | 1.924 | 5.151 | 23 | 168.75 |
| Legnica | 16.208 | 51.193 | 123 | 11 | 5.494 | 1.728 | 4.896 | 24 | 161.68 |
| Wrocław-Strachowice | 16.900 | 51.103 | 120 | 11 | 5.512 | 1.751 | 4.909 | 20 | 160.26 |
| Hel | 18.812 | 54.604 | 1 | 29.5 | 5.917 | 2.244 | 5.24 | 27 | 154.15 |
| Warszawa-Okęcie | 20.961 | 52.163 | 106 | 10 | 5.678 | 1.97 | 5.03 | 18 | 152.12 |
| Chojnice | 17.533 | 53.715 | 164 | 15 | 5.579 | 2.008 | 4.94 | 22 | 140.72 |
| Mława | 20.361 | 53.104 | 147 | 10.7 | 5.362 | 1.85 | 4.76 | 20 | 137.45 |
| Leszno | 16.535 | 51.836 | 91 | 16 | 5.246 | 1.823 | 4.66 | 23 | 131.72 |
| Krosno | 21.769 | 49.707 | 330 | 10 | 5.23 | 1.976 | 4.64 | 19 | 115.80 |
| Ślubice | 14.619 | 52.349 | 53 | 10 | 5.232 | 2.112 | 4.63 | 23 | 111.53 |
| Lublin-Radawiec | 22.394 | 51.217 | 238 | 10.2 | 5.01 | 1.862 | 4.45 | 79 | 110.15 |
| Mikołajki | 21.589 | 53.789 | 127 | 18.4 | 5.174 | 2.121 | 4.58 | 23 | 106.91 |
| Suwałki | 22.949 | 54.131 | 184 | 15 | 5.081 | 2.041 | 4.50 | 19 | 104.70 |
| Szczecin | 14.623 | 53.395 | 1 | 24.1 | 4.906 | 1.995 | 4.35 | 24 | 98.00 |
| Katowice-Muchowiec | 19.033 | 50.241 | 278 | 10 | 4.639 | 1.71 | 4.14 | 18 | 97.30 |
| Jelenia Góra | 15.789 | 50.900 | 342 | 16 | 4.264 | 1.526 | 3.84 | 21 | 90.37 |
| Gorzów Wielkopolski | 15.277 | 52.741 | 71 | 10 | 4.857 | 2.197 | 4.30 | 21 | 85.94 |
| Lesko | 22.342 | 49.466 | 420 | 10 | 4.575 | 1.815 | 4.07 | 20 | 84.88 |
| Siedlce | 22.245 | 52.181 | 152 | 11.8 | 4.608 | 1.955 | 4.09 | 18 | 81.77 |
| Opole | 17.969 | 50.627 | 163 | 10 | 4.416 | 1.834 | 3.92 | 18 | 77.28 |

Table 2. Cont.

| Station | Longitude (E) | Latitude (N) | H _{station} ASL | H _{anemometer} AGL | c | k | V _{average} | V _{max gust} | WPD |
|--------------|---------------|--------------|--------------------------|-----------------------------|-------|-------|----------------------|-----------------------|---------------------|
| - | [°] | [°] | [m] | [m] | [m/s] | [-] | [m/s] | [m/s] | [W/m ²] |
| Terespol | 23.621 | 52.078 | 133 | 11.8 | 4.629 | 2.101 | 4.10 | 17 | 77.08 |
| Zielona Góra | 15.524 | 51.930 | 192 | 11 | 4.762 | 2.314 | 4.22 | 21 | 76.56 |
| Toruń | 18.595 | 53.042 | 69 | 10 | 4.626 | 2.153 | 4.10 | 19 | 75.68 |
| Olsztyn | 20.423 | 53.771 | 133 | 16.4 | 4.514 | 2.089 | 4.00 | 21 | 71.94 |
| Kielce-Suków | 20.692 | 50.810 | 260 | 10 | 4.244 | 1.824 | 3.77 | 18 | 68.50 |
| Wieluń | 18.558 | 51.211 | 199 | 10 | 4.367 | 2.035 | 3.87 | 16 | 66.20 |
| Kozienice | 21.543 | 51.565 | 123 | 11 | 4.197 | 1.925 | 3.72 | 18 | 63.01 |
| Piła | 16.748 | 53.131 | 72 | 10 | 4.093 | 1.997 | 3.63 | 18 | 56.48 |
| Białystok | 23.162 | 53.107 | 148 | 15 | 3.728 | 2.165 | 3.30 | 16 | 39.14 |
| Zakopane | 19.960 | 49.294 | 852 | 15.1 | 3.554 | 3.298 | 3.19 | 24 | 24.68 |

Having the wind speed determined with the Weibull distribution, it is possible to calculate the average wind speed [3,9]:

$$\bar{V} = c \cdot \Gamma\left(1 + \frac{1}{k}\right) \quad (7)$$

where Γ is the gamma function, and $\Gamma(x) = \int_0^{\infty} t^{x-1} \cdot \exp(-t) dt$.

Similarly, one may express the wind power density, defined as a power of the flow passing through a unitary area [10]:

$$WPD = \frac{P}{A} = \int_0^{\infty} 0.5 \cdot \rho \cdot V^3 \cdot f(V) dV = 0.5 \cdot \rho \cdot c^3 \cdot \Gamma\left(1 + \frac{3}{k}\right) \quad (8)$$

The abovementioned equation may be re-formulated using the average wind speed [9]:

$$WPD = 0.5 \cdot \rho \cdot \bar{V}^3 \cdot \frac{\Gamma\left(1 + \frac{3}{k}\right)}{\left[\Gamma\left(1 + \frac{1}{k}\right)\right]^3} \quad (9)$$

Air density is typically calculated using the Clapeyron's ideal gas law, assuming that the air is dry. However, if the air humidity is significant, it can be also included. The air density is then given by the following equation:

$$\rho = \frac{p_{atm}}{r_{dry} \cdot (T + 273.15)} - \frac{RH \cdot a \cdot e^{\left(\frac{bT}{T+c}\right)}}{r_{dry} \cdot (T + 273.15)} + \frac{RH \cdot a \cdot e^{\left(\frac{bT}{T+c}\right)}}{r_{vap} \cdot (T + 273.15)} \quad (10)$$

As has been presented in Figure 4, the air density is mostly related with the temperature and, in a smaller part, with the humidity (especially in higher temperatures) and pressure. However, due to the range of variation in these parameters over the year, the resultant parameter may be assumed as constant. Commonly, the value of 1.225 kg/m³ is applied, but in the presented study, the mean value for each station has been assumed.

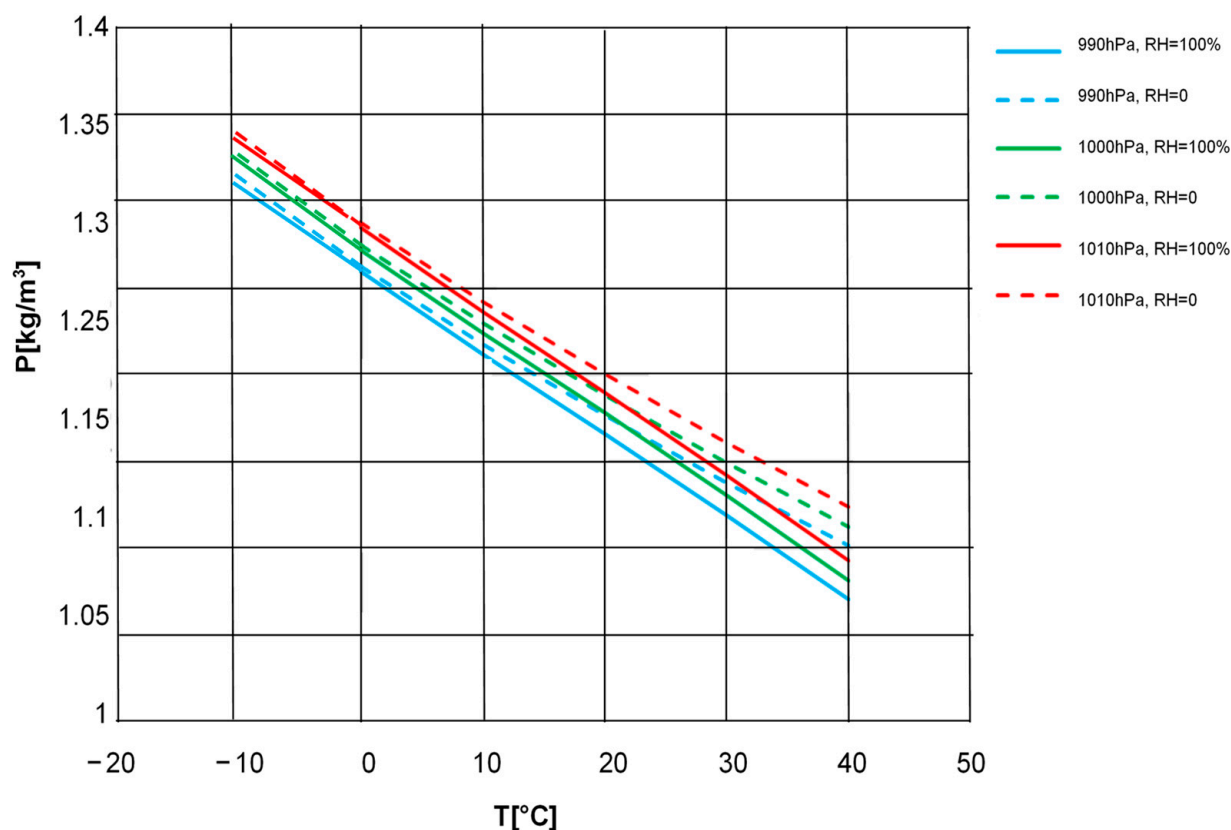


Figure 4. Air density as a function of temperature, pressure and humidity.

3. Results

The wind power density calculated according to Equation (8) has been presented on the map of Poland. The map has been performed using Inverse Distance interpolation method. Two stations have been removed: Śnieżka and Kasprowy Wierch, both of which are located in the southern part of Poland, in high mountains and on a top of the mountain. Thus, the wind speed located by these stations is highly specific and eventually interferes with the mesoscale picture of the WPD distribution. As a result, the data achieved in 49 synoptical stations have been exploited.

The analysis of the wind power density map (Figure 5) shows at the first glance that the maximum values have been observed in the northern part, along the shore of Baltic Sea. This is clearly caused by the greatest wind speed values, observed in this area for years. However, the distribution is strongly nonuniform: the greatest energy of 591 W/m^2 is captured by the Kołobrzeg-Dźwirzyno station (where the estimated average wind speed exceeded 7.5 m/s), whereas for neighboring stations, Łeba and Ustka, the WPD is greater than 400 W/m^2 (the wind speed is slightly below 7.0 m/s). Clearly, one can observe that the slight difference in average speed gave a significant difference in wind power density. It must be underlined, however, that the anemometer in Kołobrzeg is located two times lower the height above the ground than in adjacent stations. Thus, the Hellman's law factor increased from 1.32 to 1.52. However, the overall data analysis showed that WPD and Hellman's law factor are poorly correlated ($R^2 = 0.016$), which would suggest that the results are distorted due to standardization of the height AGL to 100 m.

On the other hand, the values of wind power density achieved for other stations on the Baltic Sea shore (Hel— 154 W/m^2 , Gdańsk— 178 W/m^2 , Koszalin— 169 W/m^2) prove that one may not claim that the seashore locations have the greatest WPD. Looking at the mesoscale map may be confusing.

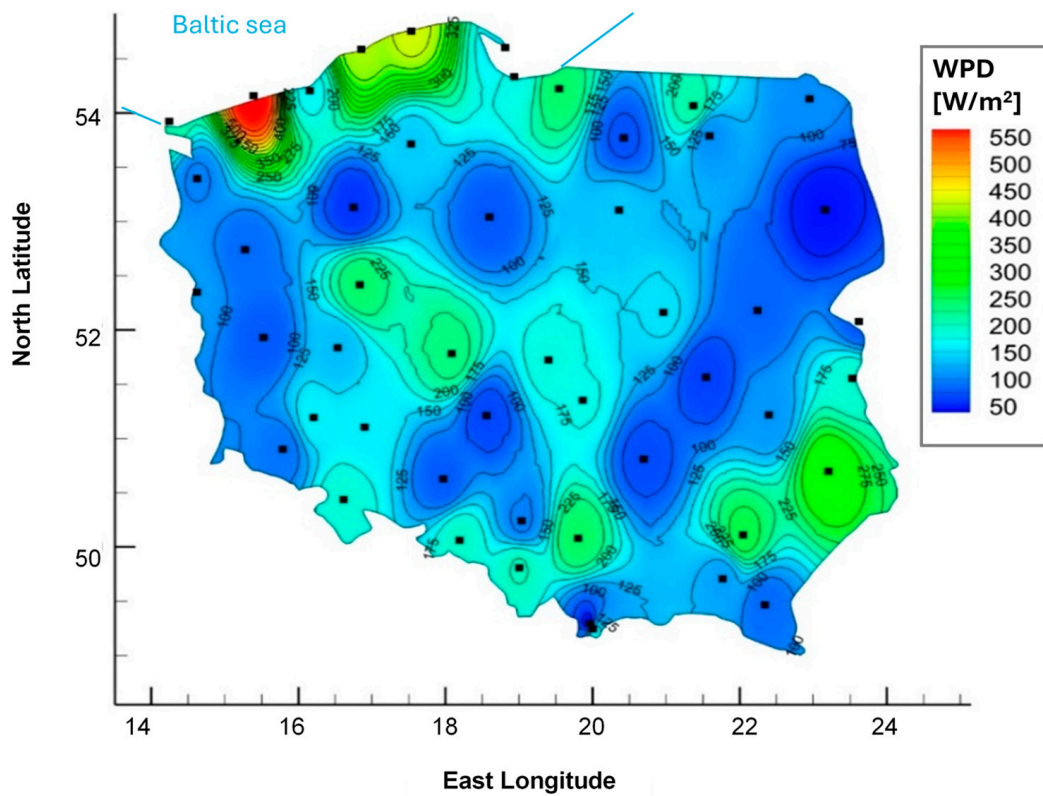


Figure 5. Distribution of the wind power density [W/m²] in Poland.

It also must be noted that the range of wind power density across Poland is more than significant. The lowest achieved value for Zakopane station is only 24 W/m², which makes up only 4% of the maximum value. The statistics of calculated WPD values have been presented in Figure 6 and in numerical form in Table 2, jointly with the coefficients of the Weibull distribution for each included station. Moreover, Table 2 also includes the maximum speed of wind (gust) and the average speed of wind, calculated with Equation (7). The latter parameter has been also plotted in Figure 7.

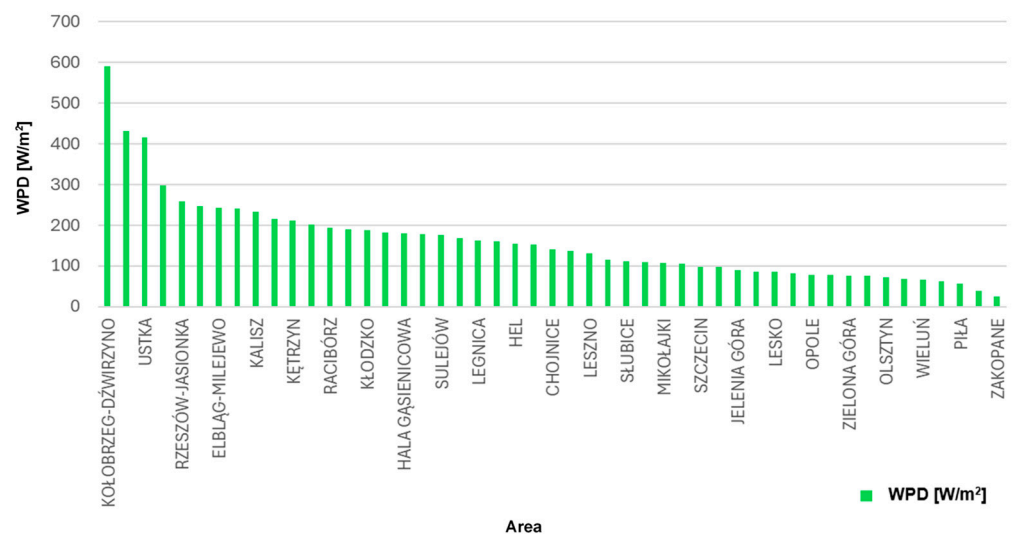


Figure 6. Wind power density for various stations.

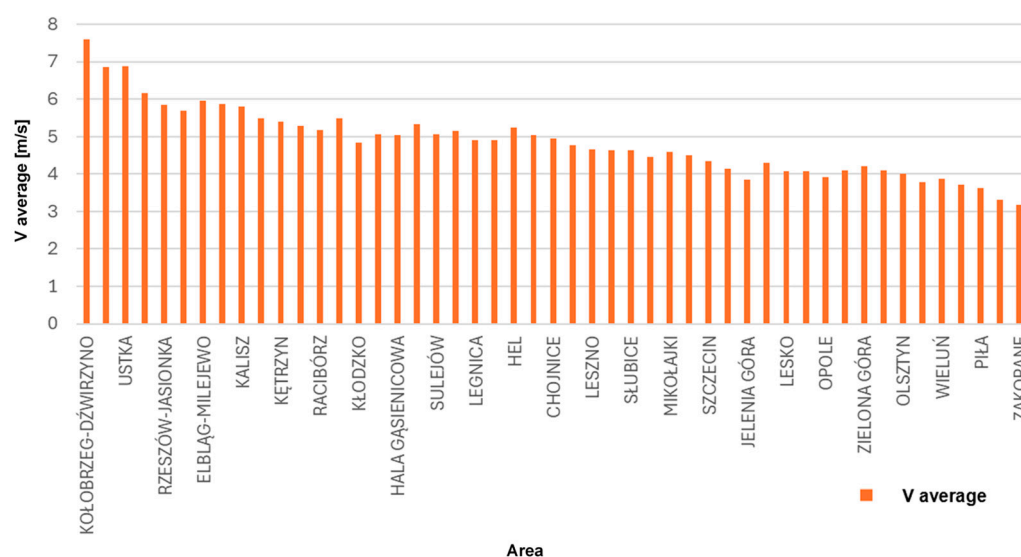


Figure 7. Average wind speed for various stations.

4. Wind Power Density Versus Wind Turbine Energy

The wind power density map shows the benefit of locating the wind turbine on the seashore—at least in some places, since some stations achieved moderate WPD values. Among the second best are the locations in south-eastern Poland (Zamość, Rzeszów—values of about 300 W/m^2 and 260 W/m^2 , respectively). Similarly, above-average wind power density has been calculated for some locations in Greater Poland (Poznań— 240 W/m^2 , Kalisz— 230 W/m^2). The average wind power density for all included stations equals 160 W/m^2 .

The wind power density, presented and discussed in this paper, obviously shows the amount of energy that can potentially be utilized to power the wind turbine. However, the consumable energy harvested by the wind turbine would be significantly lower. The efficiency of the wind turbine is defined as the Betz coefficient, named after the German engineer, Albert Betz, who introduced this fundamental equation in 1919 which was published shortly after in [34]:

$$C_p = \frac{P_{\text{turbine}}}{P_{\text{wind}}} \quad (11)$$

According to Betz, the efficiency of the wind turbine can be assessed using the Rankine–Froude actuator disk theory, which defines the flow through a rotor as a uniform, single-dimensional, axisymmetric and steady flow. Obviously, the rotor is simplified to an infinitely thin disc, with no hub nor blades; consequently, no torque is introduced in this model. The diameter and speed of the flow varies with the distance from the rotor. Such assumptions make the expression of the power consumed by the wind turbine very easy:

$$P_{\text{turbine}} = F \frac{dx}{dt} = \rho \cdot A_T \cdot V^2 (V_1 - V_2) \quad (12)$$

where index “1” refers to the cross section far in front of the rotor disc (upstream) and index “2” far behind it (downstream), and parameters with no index refer to the disc position. Similarly, the power of the wind may be expressed as

$$P_{\text{wind}} = \frac{1}{2} \rho \cdot A_T \cdot V^3 \quad (13)$$

Eventually, it is easy to show that the Betz coefficient may be expressed as

$$C_p = (1 - \mu^2)(1 + \mu) \quad (14)$$

where μ is the “interference factor”, a ratio of velocities downstream and upstream:

$$\mu = \frac{V_2}{V_1} \quad (15)$$

Clearly, the $C_p(\mu)$ function is a third-order parabola with a single local maximum in the range of μ between 0 and 1. It is easy to check that differentiating the Equation (14) gives a non-trivial solution of the optimum value of the interference factor:

$$\mu_{opt} = \frac{1}{3} \quad (16)$$

It is easy to check that the maximum value of the Betz coefficient is equal to $16/27 = 59.26\%$. This value is referred as the Betz Limit or Betz Criterion, and despite it having been formulated over a century ago, it remains valid for all types of wind turbines. On the other hand, it is only a theoretical maximum value, which does not include air flow friction, blade roughness and all other energy losses. Modern wind turbines reach lower practical values of maximum efficiency, at around 40% [35]. The efficiency of different types of wind turbines has been plotted in Figure 8. The X-axis represents a tip speed ratio (TSR):

$$TSR = \frac{\text{blade's tip speed}}{\text{wind speed}} = \frac{\omega R}{V} \quad (17)$$

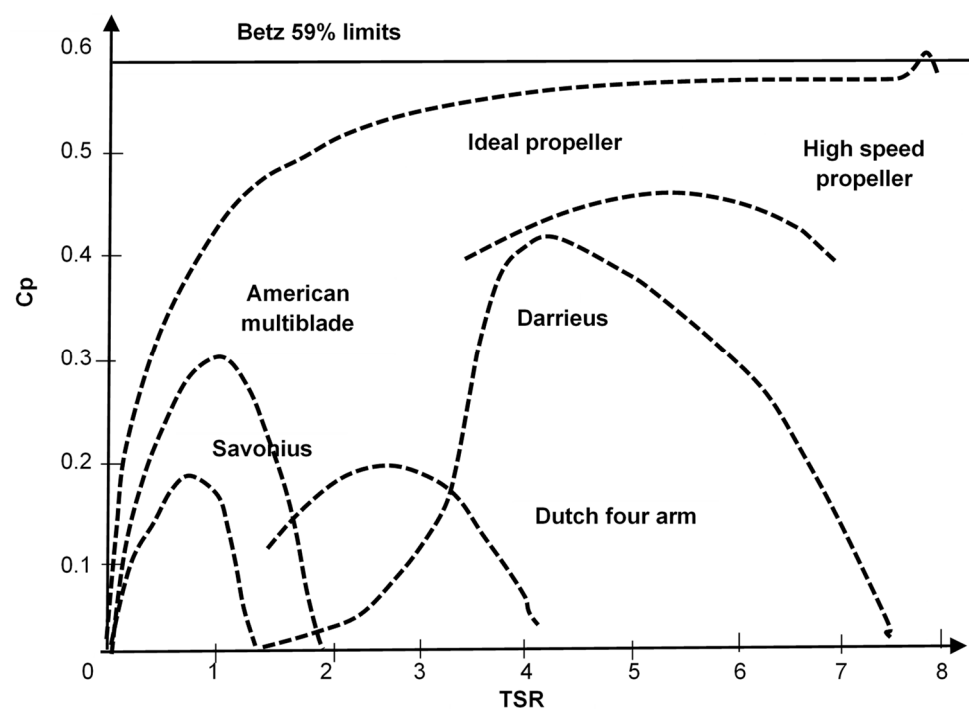


Figure 8. The power coefficient as a function of the tip speed ratio [35,36].

On the other hand, the tip speed ratio is a nondimensional coefficient, which defines the turbine operating point, but it is not measured directly. The TSR depends on wind speed and the revolution speed of the turbine, which is also affected by the wind speed and turbine settings (like blades pitch angle). Thus, it is convenient to analyze the C_p plotted directly versus wind speed; see Figure 9. To track the maximum power point, the generator controls the angular speed of the rotor shaft, and this is performed by controlling the generator currents (electrical control) [37–39]. Clearly, the Betz coefficient reaches its maximum at a wind speed of about 8 m/s in the presented example, but this depends, among others, on the turbine settings, on the blades’ pitch angle, as well as on the aerodynamic characteristics of the blades airfoil (and eventually, the blade itself), including

lift and the lift-to-drag ratio versus the angle of attack. However, it must be underlined that, in practical applications, the turbine setting is somehow controlled. To track the maximum power point, the generator controls the angular speed of the rotor shaft, and this is performed by controlling the generator currents (electrical control). Secondly, to ensure the safety of the turbine if the wind speed limit (upper cut-off speed) is exceeded, the power, torque and angular speed of the turbine is limited. In this case, two control strategies are typically implemented [40]: blade pitch control and stall control. In the first case, the blade pitch is reduced by a hydraulic actuator or an electric stepper motor, to reduce the lift coefficient which powers the rotor's revolution. Meanwhile, stall-controlled turbines use passive control systems, i.e., the blades' geometry is designed to direct the wake behind one blade towards another one, if the wind speed achieves its limit.

If we assume that Figure 9 covers an exemplary wind turbine that may be implemented, it is worthwhile for us to compare its performance with the wind characteristics. To do so, we marked the range of the average wind speed in Poland as presented in the previous section. It is clearly visible that the optimal speed for such a turbine (in terms of maximum C_p), which is about 8 m/s, is close to the maximum average wind speed available in Poland, mostly for seashore locations: the average speed calculated for Kołobrzeg-Dźwirzyno, Łeba and Ustka are in range from 6.5 m/s to 7.5 m/s. Knowing the probability distribution of the wind speed in exact localization would allow us to set the average speed as a design point of the blade.

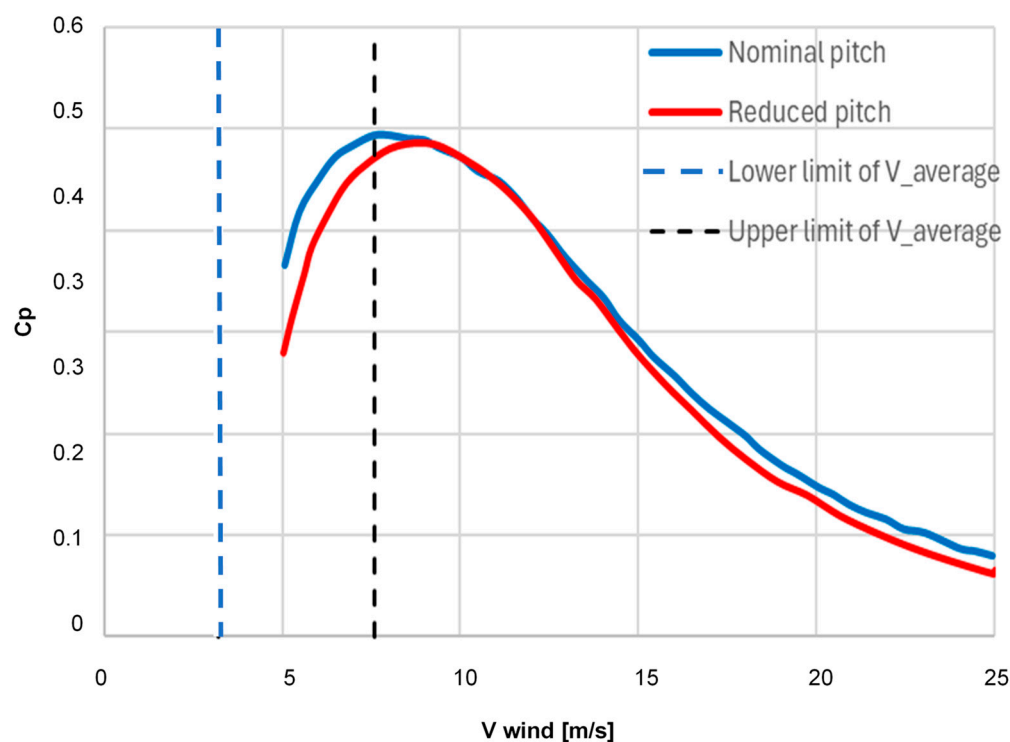


Figure 9. Range of average wind speed achieved in Poland, compared with power coefficient of the exemplary 2 MW wind turbine, as a function of the wind speed [40,41].

However, a detailed analysis of the Betz coefficient is crucial in terms of blade optimization; one should not forget that the actual output power of the turbine is a factor of this coefficient and the wind power, which in line is proportional to the third power of the wind speed, and this relation is dominant. Eventually, the power output versus wind speed gives us a well-known power curve (Figure 10).

The turbine should operate with the highest efficiency as the wind speed increases to the nominal/rated value. In this case, the power output becomes the maximum from the generator's point of view; thus, it should not be further increased [42,43]. Pitch-controlled

turbines maintain a constant level of the power, while stall-controlled ones are designed such that the rotor efficiency “collapses” at high wind speeds. Due to the blade design, this behavior is intrinsic, and no active control systems are required to achieve the aerodynamic efficiency reduction [40] (Figure 10).

If the range of average wind speeds is marked on the power curve of a generic turbine (Figure 10), it becomes evident that the wind turbines in Poland should be optimized in terms of low wind speed. The lowest value of the average wind speed (3.19 m/s, achieved for Zakopane station) is close to the lower cut-off speed of the presented turbine. That means that this turbine would barely move, and the generated power would be insufficient. What is more, only the slightly higher values have been obtained for Białystok and Piła (3.3 m/s and 3.63 m/s, respectively). All these stations are located in different parts of Poland: Zakopane is located in Tatry mountain, in the southern part of the country, and Białystok lies in north-eastern part of Poland and Piła, in the western part of the country; the two latter cases cover plain, lowland areas. In this case, an orographic variation in wind speed is not very probable. Thus, the risk of insufficient power supplied by the wind turbine is relatively high. Nevertheless, even in the case of most windy areas, the exemplary turbine would be, on average, utilized at roughly 20% of its nominal power. Again, precise estimation of wind speed probability for a given localization would be needed to clarify these values and estimate the rated power that would be needed.

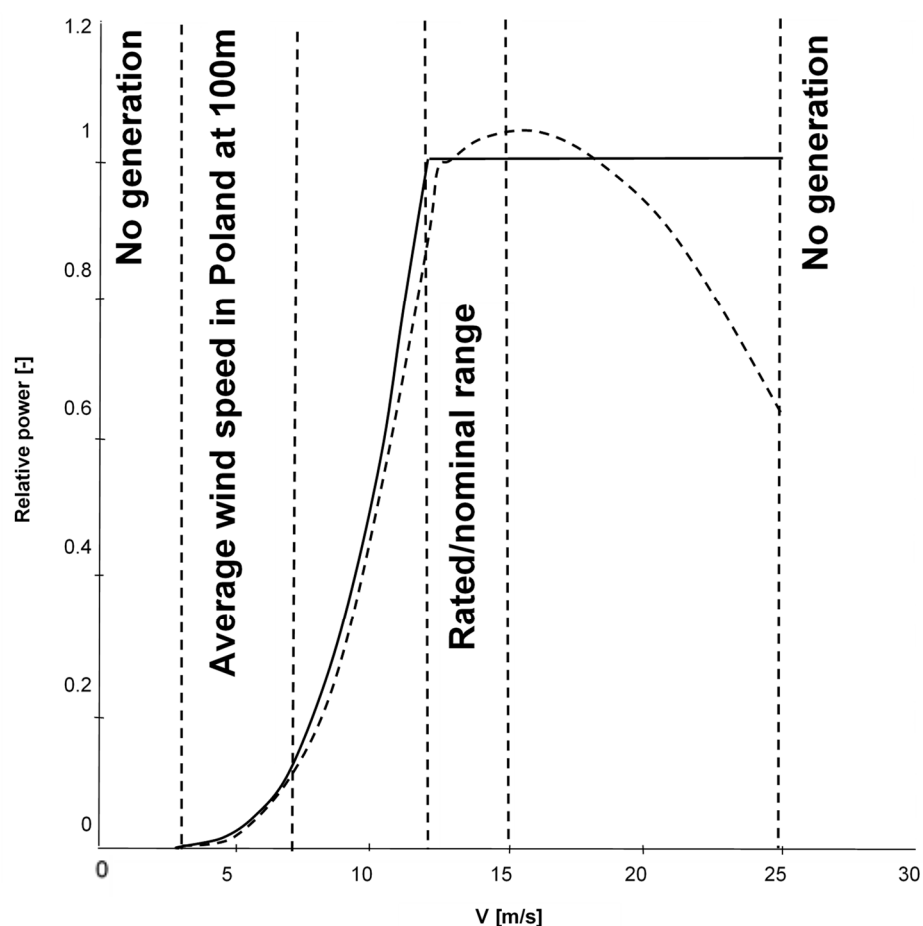


Figure 10. Exemplary power curve for pitch-controlled (solid line) and stall-controlled (dashed line) wind turbines [43].

5. Conclusions

The aim of the present research was to investigate the requirements that have to be met to design wind power stations that would be an optimal fit for the climatic conditions

in Poland. This study combined results of empirical studies on wind velocity distributions with the physical fundamentals of wind power station design.

The meteorological data gathered during the year 2023 in 50 synoptical stations in Poland have been utilized to calculate the yearly wind power density (per unitary area), at a height of 100 m above ground level (AGL). The average value of WPD is 160 W/m^2 , but the variety in the range is significant. The greatest values have been observed in some places on the Baltic Sea shore (a maximum of 591 W/m^2 has been observed in Kołobrzeg-Dźwirzyno) and a minimum value of 24 W/m^2 in Zakopane.

The resultant WPD values plotted on the map of Poland show that no evident mesoscale trend is visible. In spite of this, the energy output of a hypothetical wind turbine may be assessed using the Weibull probability distribution based on the SYNOP data gathered in adjacent stations. The coefficients of such distributions has been presented in this paper.

To calculate the output energy, it is not enough to estimate WPD and wind speed probability. One must also estimate the power curve (power versus wind speed) or Betz coefficient versus wind speed; both these functions depend strongly on the wind turbine design. Setting the cut-off speeds (lower and upper) can be easily included in the energy estimation, which eases a trade-off between exploited energy and the strength and costs of the turbine. The statistical data can be utilized as well, not only as a Weibull distribution, but also as a Gumbel distribution which defines the probability of maximum wind speed.

As indicated in the results of wind velocity measurements, in most commonly observed cases, the wind speed in Poland is approximately 5 to 7 m/s. Therefore, it is necessary to look for solutions for turbines to operate optimally at low wind speeds.

The study presented in this paper concerns the integrated (total) values of energy, which can be achieved across the whole year. However, it must be underlined that, in reality, this value varies from month to month or even during the day. For instance, the measurements of wind speed during the year showed that in most meteorological stations in Poland, the highest wind speed values were achieved during the winter, from December to March. Meanwhile, the lowest values have been recorded in July and August [44]. Furthermore, the daily variation in wind speed is also clearly observable. Koźmiński and Michalska in [45] have compared measurements taken at 7:00 a.m., 1:00 p.m. and 9:00 p.m. According to that, the greatest wind speed has been observed around noon, especially in the spring, from March to May. In the morning, the wind is significantly weaker, and in the evening, it is the weakest. The monthly variation in wind speed is the greatest in February, March and September, while in January, May and June, the variation coefficient decays. These variations have been included in the presented results, as the calculation of wind power density relies on frequently gathered measurements. On the other hand, as the WPD is strongly related with the wind speed (in the third power), one may estimate that the variation in the presented values in late winter or in September will be the highest. It would be beneficial to express this variation quantitatively, by applying the time-dependency of the wind speed probability distribution, or by using the gathered data directly to estimate the standard deviation as a metric of daily variation or monthly variation. These can eventually be used to study the 'reliability' of the wind turbine: what is the percentage of time when the supplied power may be efficiently consumed? Such studies exceed the scope of the following paper but can be performed in the future.

Author Contributions: Conceptualization, P.R., O.O., K.T. and A.W.; methodology, P.R., O.O. and K.T.; software, O.O., P.R., A.W. and K.T.; validation, P.R., M.Z. and O.O.; formal analysis, P.R., O.O. and K.T.; investigation, P.R., A.W., M.Z. and O.O.; data curation, P.R., O.O., K.T. and A.W.; writing—original draft preparation, P.R., O.O. and K.T.; writing—review and editing, O.O., P.R. and K.T.; visualization, P.R., A.W., O.O. and K.T.; supervision, P.R., O.O., M.Z. and K.T. All authors have read and agreed to the published version of the manuscript.

Funding: This study was financed by the Bialystok University of Technology under the project WZ/WIZ-INZ/4/2022 (Olga Orynycz), conducted in part during cooperation stays in the Łukasiewicz Institute of Aviation, Warsaw, 2023.

Data Availability Statement: This study did not report any data.

Conflicts of Interest: The authors declare no conflicts of interest.

References

1. Caban, J.; Małek, A.; Šarkan, B. Strategic Model for Charging a Fleet of Electric Vehicles with Energy from Renewable Energy Sources. *Energies* **2024**, *17*, 1264. [CrossRef]
2. Derkacz, A.J.; Dudziak, A.; Stopka, O.; Stopková, M. Profitability Determinants of Transport Service and Warehouse Enterprises: A Case Study from Poland. *Period. Polytech. Transp. Eng.* **2023**, *51*, 275–286. [CrossRef]
3. Lotko, W.; Smigins, R.; Tziourtzioumis, D.; Górska, M. Environmental Aspects of a Common Rail Diesel Engine Fuelled with Biodiesel/Diesel Blends. *Adv. Sci. Technol. Res. J.* **2022**, *16*, 192–201. [CrossRef]
4. Kurczyński, D.; Łagowski, P.; Wcisło, G. Experimental study into the effect of the second-generation BBuE biofuel use on the diesel engine parameters and exhaust composition. *Fuel* **2021**, *284*, 118982. [CrossRef]
5. Waluś, K.J.; Warguła, Ł. Experimental Research on Kinematic Features of Agricultural Tractor Movement on Asphalt Pavement. Available online: https://www.matec-conferences.org/articles/mateconf/pdf/2022/04/mateconf_mms2020_05005.pdf (accessed on 19 February 2024).
6. Peng, B.; Streimikiene, D.; Agnusdei, G.P.; Balezentis, T. Is sustainable energy development ensured in the EU agriculture? Structural shifts and the energy-related greenhouse gas emission intensity. *J. Clean. Prod.* **2024**, *445*, 141325. [CrossRef]
7. Ovaere, M.; Proost, S. Cost-effective reduction of fossil energy use in the European transport sector: An assessment of the Fit for 55 Package. *Energy Policy* **2022**, *168*, 113085. [CrossRef]
8. GlobEnergia. Germany Produced More Than 50% of Electricity from RES in 2023! Available online: <https://globenergia.pl/niemcy-wyprodukowali-ponad-50-energii-elektrycznej-z-oze-w-2023/> (accessed on 19 February 2024).
9. GlobEnergia. Portugal with Record Share of RES in Electricity Generation! Available online: <https://globenergia.pl/portugalia-z-rekordowym-udzialem-oze-w-generacji-pradu/> (accessed on 19 February 2024).
10. GlobEnergia. Wind in Sails for Offshore Wind Farms in Poland! Available online: <https://globenergia.pl/wiatr-w-zagle-dla-morskich-elektrowni-wiatrowych-w-polsce/> (accessed on 19 February 2024).
11. TouchWind. Consortium Starts Demonstration Project into Positive Wake Effects of TouchWind’s Floating Wind Turbine. Available online: <https://touchwind.org/news/consortium-starts-demonstration-project-into-positive-wake-effects-of-touchwinds-floating-wind-turbine/> (accessed on 19 February 2024).
12. Vestas. Wind Turbine Product Portfolio. Available online: <https://us.vestas.com/en-us/products> (accessed on 19 February 2024).
13. Tests to Begin on a Counter-Rotating Floating Offshore Wind Turbine Concept. Available online: <https://maritime-executive.com/article/tests-to-begin-on-a-counter-rotating-floating-offshore-wind-turbine-concept> (accessed on 19 February 2024).
14. GE Renewable Energy. Haliade-X Offshore Wind Turbine. Available online: <https://www.ge.com/renewableenergy/wind-energy/offshore-wind/haliade-x-offshore-turbine> (accessed on 19 February 2024).
15. GE Renewable Energy. Cypress Onshore Wind Turbine Platform. Available online: <https://www.ge.com/renewableenergy/wind-energy/onshore-wind/cypress-platform> (accessed on 19 February 2024).
16. Siemens Gamesa. SG 14-222 DD: The Winds of Change Have Never Been Stronger. Available online: <https://www.siemensgamesa.com/products-and-services/offshore/wind-turbine-sg-14-222-dd> (accessed on 19 February 2024).
17. Li, D.; Zhang, Z.; Zhou, X.; Zhang, Z.; Yang, X. Cross-wind dynamic response of concrete-filled double-skin wind turbine towers: Theoretical modelling and experimental investigation. *J. Vib. Control* **2023**, 1–13. [CrossRef]
18. VENTUS Power Generator. Products & Services. Available online: <https://ventus.group/products-services> (accessed on 19 February 2024).
19. EnVentus Platform Variants. Available online: <https://www.vestas.com/en/products/enventus-platform> (accessed on 19 February 2024).
20. Polish Wind Power Plants. Available online: <https://generatory-wiatrowe.pl/produkty/polskie-elektrownie-wiatrowe/> (accessed on 19 February 2024).
21. Bošnjaković, M.; Katinić, M.; Santa, R.; Marić, D. Wind Turbine Technology Trends. *Appl. Sci.* **2022**, *12*, 8653. [CrossRef]
22. Żurański, J.A.; Jaśpińska, B. Directional analysis of extreme wind speeds in Poland. *J. Wind Eng. Ind. Aerodyn.* **1996**, *66*, 13–20. [CrossRef]
23. Simiu, E.; Scanlan, R.H. *Wind Effects on Structures: An Introduction to Wind Engineering*, 2nd ed.; John Wiley and Sons: New York, NY, USA, 1986.
24. Gumbel, E.J. *Statistics of Extremes*, 1st ed.; Columbia University Press: New York, NY, USA, 1958. [CrossRef]
25. Chmielewski, T.; Bońkowski, A.P. Wind as a natural hazard in Poland. *Nat. Hazards Earth Syst. Sci.* **2023**, *23*, 3839–3844. [CrossRef]
26. Lorenc, H. *Maksymalne Prędkości Wiatru w Polsce*, 1st ed.; Instytut Meteorologii i Gospodarki Wodnej: Warszawa, Polska, 2012; pp. 5–94. Available online: <https://bibliotekanauki.pl/books/2049055> (accessed on 19 February 2024).
27. Belu, R. Assessment and Analysis of Offshore Wind Energy Potential. Available online: <https://www.intechopen.com/chapters/74556> (accessed on 19 February 2024).
28. Wei, J.; Hulio, Z.H.; Rashid, H. Site specific assessment of wind characteristics and determination of wind loads effects on wind turbine components and energy generation. *Int. J. Energy Sect. Manag.* **2018**, *12*, 341–363. [CrossRef]

29. Harris, R.I.; Cook, N.J. The parent wind speed distribution: Why Weibull. *J. Wind Eng. Ind. Aerodyn.* **2014**, *131*, 72–87. [CrossRef]
30. Jung, C.; Schindler, D.; Laible, J.; Buchholz, A. Introducing a system of wind speed distributions for modeling properties of wind speed regimes around the world. *Energy Convers. Manag.* **2017**, *144*, 181–192. [CrossRef]
31. Kowalik-Pilarska, E. Wind Speed Parameters Estimation for Poland as a Result of Mesoscale Modelling. Available online: http://www.phd4gen.pl/wp-content/uploads/2021/06/22_06_2021_EKP_UZ3.pdf (accessed on 19 February 2024).
32. Banuelos-Ruedas, F.; Camacho, C.A.; Rios-Marcuello, S. Methodologies Used in the Extrapolation of Wind Speed Data at Different Heights and Its Impact in the Wind Energy Resource Assessment in a Region. In *Wind Farm—Technical Regulations, Potential Estimation and Siting Assessment*; Intechopen: London, UK, 2011. Available online: <https://www.intechopen.com/chapters/17121> (accessed on 19 February 2024). [CrossRef]
33. PN-EN 1991-1-4; Impact on Constructions. The Effects of Wind. Available online: https://wiedza.pkn.pl/documents/28503/0/Eurokody_wprowadzenie_tablica_wrzesie%C5%84_2018.pdf/f91c2e0f-9b08-4d7c-96ed-2af3a5f57602 (accessed on 19 February 2024).
34. Betz, A. *Wind-Energie und Ihre Ausnutzung durch Windmühlen*; Vandenhoeck und Ruprecht: Göttingen, Germany, 1926.
35. Ragheb, M.; Ragheb, A.M. Wind Turbines Theory—The Betz Equation and Optimal Rotor Tip Speed Ratio. Available online: https://cdn.intechopen.com/pdfs/16242/InTechWind_turbines_theory_the_betz_equation_and_optimal_rotor_tip_speed_ratio.pdf (accessed on 19 February 2024).
36. Santiago, G.; Hernandez, W.; Costa De Araujo, A.C.; Rosa, M.; González, M. Application of Product Development Process (PDP) in the Construction of Vertical Axis Wind Turbine with Movable Blades. Available online: https://www.academia.edu/42937714/Application_of_product_development_process_PDP_in_the_construction_of_vertical_axis_wind_turbine_with_movable_blades (accessed on 19 February 2024).
37. Wind Turbine Control Methods. Available online: <https://www.ni.com/en/solutions/energy/condition-monitoring/wind-turbine-control-methods.html> (accessed on 31 May 2024).
38. Flores, D.R.L.; Gómez, J.A.P.; Herrera, R.; Alvarado, M.S. Tracking Control of the Maximum Power Point (MPPT) in A Small Wind Turbine (SWT) for Isolated Residential Applications. *Wseas Trans. Circuits Syst.* **2013**, *8*, 253–261.
39. Muñoz-Palomeque, E.; Sierra-García, J.E.; Santos, M. Wind turbine maximum power point tracking control based on unsupervised neural networks. *J. Comput. Des. Eng.* **2023**, *10*, 108–121. [CrossRef]
40. Mihet-Popa, L.; Groza, V. Dynamic modeling, simulation and control strategies for 2 MW wind generating systems. *Int. Rev. Model. Simul.* **2010**, *3*, 1410–1418.
41. Heier, S. *Grid Integration of Wind Energy: Onshore and Offshore Conversion Systems*, 1st ed.; John Wiley and Sons: New York, NY, USA, 1998.
42. Koźmiński, C.; Michalska, B. Characterization of wind speed and calms in Poland. *Acta Agrophysica* **2002**, *78*, 111–132. Available online: <https://agro.icm.edu.pl/agro/element/bwmeta1.element.agro-article-18ec9a36-3a7d-4f1d-8490-7a7ed28bfc05> (accessed on 19 February 2024).
43. Hansen, L.H.; Helle, L.; Blaabjerg, F.; Ritchie, E.; Munk-Nielsen, S.; Binder, H.; Sorensen, P.; Bak-Jensen, B. *Conceptual Survey of Generators and Power Electronics for Wind Turbines*; Riso-r-1205(EN); Riso National Laboratory: Roskilde, Denmark, 2001. Available online: <https://www.osti.gov/etdweb/biblio/20262554> (accessed on 19 February 2024).
44. Zöldy, M.; Baranyi, P.; Török, Á. Trends in Cognitive Mobility in 2022. *Acta Polytech. Hung.* **2024**, *21*, 189–202. [CrossRef]
45. Strijhak, S.V.; Gergel, V.P.; Ivanov, A.V.; Gadal, S.Z. On the Problem of Choosing the Optimal Parameters for the Wind Farm in the Arctic Town of Tiksi. In *Mathematical Modeling and Supercomputer Technologies*; MMST 2020. Communications in Computer and Information Science, 1413; Springer: Cham, Switzerland, 2021. Available online: <https://amu.hal.science/hal-03274909> (accessed on 19 February 2024). [CrossRef]

Disclaimer/Publisher’s Note: The statements, opinions and data contained in all publications are solely those of the individual author(s) and contributor(s) and not of MDPI and/or the editor(s). MDPI and/or the editor(s) disclaim responsibility for any injury to people or property resulting from any ideas, methods, instructions or products referred to in the content.